Collision Risk Mitigation in Geostationary Orbit

Article *in* Space Debris · June 2000

DOI: 10.1023/A:1021255523174

2 authors:

Luciano Anselmo
Italian National Research Council

C. Pardini
Italian National Research Council

COLLISION RISK MITIGATION IN GEOSTATIONARY ORBIT

L. ANSELMO and C. PARDINI

Consiglio Nazionale delle Ricerche (CNR) – CNUCE Institute, Spaceflight Dynamics Section, CNUCE/CNR, Via Moruzzi 1, 56124 Pisa (PI), Italy (Tel.: +39-050-315-2952; Fax: +39-050-313-8091; E-mail: Luciano.Anselmo@cnuce.cnr.it)

(Received 31 October 2001; Accepted 2 March 2002)

Abstract. The short- and long-term effects of spacecraft explosions, as a function of the end-of-life re-orbit altitude above the geostationary orbit (GEO), were analyzed in terms of their additional contribution to the debris flux in the GEO ring. The simulated debris clouds were propagated for 72 yrs, taking into account all the relevant orbital perturbations.

The results obtained show that 6–7 additional explosions in GEO would be sufficient, in the long term, to double the current collision risk with sizable objects in GEO. Unfortunately, even if spacecraft were to re-orbit between 300 and 500 km above GEO, this would not significantly improve the situation. In fact, an altitude increase of at least 2000 km would have to be adopted to reduce by one order of magnitude the long-term risk of collision among geostationary satellites and explosion fragments. The optimal debris mitigation strategy should be a compromise between the reliability and effectiveness of spacecraft end-of-life passivation, the re-orbit altitude and the acceptable debris background in the GEO ring. However, for as long as the re-orbit altitudes currently used are less than 500 km above GEO, new spacecraft explosions must be avoided in order to preserve the geostationary environment over the long term.

Keywords: collision risk, debris flux, geostationary ring, orbital perturbations, satellite explosions, satellite re-orbiting

Abbreviations: ASAP – Artificial Satellite Analysis Program; ASI – Agenzia Spaziale Italiana (Italian Space Agency); CLDSIM – cloud debris simulator; CNUCE – former Centro Nazionale Universitario di Calcolo Elettronico; CODRM-99 – 1999.0 CNUCE Orbital Debris Reference Model; GEO – geostationary orbit; IADC – Inter-Agency Space Debris Coordination Committee; JPL – Jet Propulsion Laboratory; SDIRAT – Space Debris Impact Risk Analysis Tool; yr – year.

1. Introduction

Due to the rapid increase in the number of spacecraft and apogee kick motors in the geo-synchronous region, there was growing concern in the 1980s regarding the possible overcrowding of the geostationary orbit (GEO) and the consequent threat to its long-term utilization and exploitation (Hechler and Van der Ha, 1981; Fusco and Buratti, 1984). The risk of collision between space objects in GEO was estimated in order to devise affordable and effective end-of-life disposal measures, such as satellite re-orbiting (Chobotov, 1990).

Space Debris **2**, 67–82, 2002.

In the following decade, it became clear that also spacecraft and upper stage breakups contribute to the GEO debris environment. More recently, an international campaign of optical observations has confirmed the presence of a significant population of decimeter sized objects, probably generated by several undetected explosions (Africano and Schildknecht, 2000; Flury et al., 2000; Jorgensen et al., 2001; Schildknecht et al., 2001).

A few years ago, in order to preserve the GEO for future use, the Inter-Agency Space Debris Coordination Committee (IADC) proposed a re-orbiting strategy for the geostationary spacecraft at their end-of-life (IADC, 2000). They should be disposed to a region above the geostationary altitude and passivated, in order to reduce the risk of inadvertent explosions. The recommended perigee of the disposal orbit should be higher than the geostationary altitude by an amount ΔH (km) given by

$$\Delta H = 235 + C_r \times 1000 \times A/m, \tag{1}$$

where A is the satellite average cross-sectional area (m^2), m, the satellite mass (kg) and C_r, the radiation pressure coefficient, typically between 1 and 2, specifying the amount of solar radiation transmitted, absorbed and reflected by the spacecraft.

In a series of previous papers, the long-term effects of spacecraft and upper stage explosions, in terms of the additional debris density in the geostationary ring, were analyzed in detail with a new modeling approach, in particular to evaluate the effectiveness of end-of-life re-orbiting for debris mitigation (Anselmo and Pardini, 2000; Pardini and Anselmo, 2001). This work, and the associated modeling, has now been extended to include debris flux, thus making it easier to assess the long-term risk associated with explosions in, or near, GEO.

2. Explosions Simulation

In the present study, a 2000 kg spacecraft was assumed to have suffered a low intensity explosion (Su and Kessler, 1985; Reynolds, 1990) at five different heights, between 0 and 2000 km above the geostationary altitude (Tables I and II). The breakups were simulated using the cloud debris simulator (CLDSIM) software developed at the former Centro Nazionale Universitario di Calcolo Elettronico (CNUCE) (Pardini, 1995), while the fragments – 1733 with a diameter greater than 1 mm – were propagated for 72 yrs with a modified, multi-object version of the Artificial Satellite Analysis Program (ASAP) trajectory

TABLE I

Explosion altitudes above GEO

Simulation number	Altitude above GEO (km)
1	0
2	300
3	500
4	1000
5	2000

TABLE II

Characteristics of the simulated fragmentation events

Explosion epoch	11 May 1999
Explosion right ascension	298°
Explosion declination	0°
Fragments $\geq$ 1 mm	1733
Fragments $\geq$ 1 cm	1630
Fragments $\geq$ 10 cm	705
Maximum debris ΔV	1.94 km s^{-1}

predictor (Kwok, 1987), developed at the Jet Propulsion Laboratory (JPL). The perturbations taken into account were the harmonics (8×8) of the geopotential, the luni-solar third body gravitational attraction and the direct solar radiation pressure with eclipses.

Snapshots of the evolution of the debris clouds were obtained and saved at specific explosion elapsed times (0, 1, 6, 12, 18, 24, 30, 36, 42, 48, 54, 60, 66 and 72 yrs), during the 72 yrs' interval considered in the simulations. Each of these snapshots represented a population of objects that could be analyzed to extract the information sought for, in particular regarding its interaction with the GEO ring, defined as the volume of space centered on the GEO (mean altitude of 35,786 km, zero inclination), ± 75 km in altitude and $\pm 0.1^\circ$ in declination.

In order to numerically identify any intersection with the GEO ring, each object in a cloud snapshot was propagated for one full orbit, obtaining its state vector at fixed mean anomaly steps $\Delta M = 0.75^\circ$. In total, $360^\circ/\Delta M = 480$ state vectors were obtained for each object, but only those corresponding to positions inside the GEO ring were retained (i.e. between $\sim$500 and $\sim$15,000 state vectors for each cloud, soon after the explosion, depending on the breakup altitude above GEO). All these state vectors were therefore used to build, for each debris cloud snapshot, a new representative population of fictitious space objects, each weighted by a fractional sampling factor $\Delta M/360^\circ = 1/480$. This was done to obtain a set of debris populations which could be processed and analyzed using the Space Debris Impact Risk Analysis Tool (SDIRAT) (Pardini and Anselmo, 1999; 2000).

SDIRAT is a software code developed at CNUCE to assess the orbital debris impact risk on a specified target in earth orbit, in terms of flux, relative velocity, direction of the incoming particles, debris mass and diameter. Based on a new deterministic approach, it can use any debris population in input, provided that each representative particle is identified by its mass, size, weighting sampling factor and state vector at a reference epoch (Pardini and Anselmo, 1999, 2000). All this information was available, at each snapshot time, for the debris clouds simulated as described above. Thus, it was straightforward to apply SDIRAT and thereby be able to assess the impact risk on the GEO ring, both short- and long-term, due to the explosion fragments.

For the study presented in this paper, the target orbit whose collision risk was to be assessed was the geostationary one. The radial ($\Delta R = \pm 75$ km) and latitudinal ($\Delta\delta = \pm 0.1^\circ$) amplitudes of the control cells used by SDIRAT around the target orbit were chosen to be coincident with the GEO ring, as defined at the beginning of this section, while 1° of right ascension was adopted for the longitudinal amplitude ($\Delta\alpha = \pm 0.5^\circ$).

First of all, in order to obtain a benchmark to compare the effects of the simulated explosions, SDIRAT was used to estimate the collision risk for a geostationary spacecraft due to the existing debris population. For this purpose, the 1999.0 CNUCE Orbital Debris Reference Model (CODRM-99) (Pardini et al., 1998; Pardini, 2000) was employed, with the same control cells sizes previously described. Moreover, only the uncontrolled spacecraft crossing the GEO ring, plus spent upper stages and debris, were taken into account, for obvious reasons.

In the GEO region, CODRM-99 included not only the unclassified catalogued population, but also the classified satellites, inferred from the launch historical record, and many simulated objects, to account for the catalog incompleteness and the fragments produced by three explosions occurred in the past (Pardini, 2000). For these reasons, in the GEO region, the unclassified catalogued objects merely represented about 40% of the CODRM-99 population above 10 cm in diameter, not so far, at least statistically, from the most recent observational results (Jorgensen et al., 2001; Schildknecht et al., 2001).

The collision risk analysis was repeated separately for all the explosion events (5) and for the debris clouds snapshots (14) considered in the study, for a total of $5 \times 14 = 70$ runs of SDIRAT (plus one for the background population). The results obtained were then analyzed and compared with the impact risk due to the existing environment, as represented by CODRM-99, in order to assess the long-term consequences of satellite explosions in the GEO region, and to evaluate the effectiveness of the possible mitigation measures that could be adopted to preserve the geostationary ring, such as the IADC recommendations (IADC, 2000).

3. The Background Population of Uncontrolled Objects

Abandoned spacecraft, upper stages, mission-related objects and breakup fragments contribute to the orbital debris collision risk in GEO, although the typical relative and impact velocities are significantly smaller than at low altitudes (all the particles have the same statistical weight in the computation of the average relative velocity, while the average impact – or collision – velocity takes into account the fact that the debris flux on a target is proportional to both debris density and relative velocity; for more details and a quantitative definition see, e.g., Pardini and Anselmo, 1999). The results obtained with SDIRAT using the CODRM-99 population are summarized in Table III, while Figures 1–3 show the debris cross-sectional area flux as a function, respectively, of the azimuth, elevation and relative velocity, for the objects larger than 10 cm. The azimuth and elevation angles refer to the local horizontal plane in GEO.

TABLE III

Debris impact risk in GEO due to the background population

Objects diameter	Average relative velocity (m s^{-1})	Average impact velocity (m s^{-1})	Cross-sectional area flux (m^{-2} yr^{-1})
$\geq$10 cm	136	807	6.649×10^{-9}
$\geq$1 cm	235	1234	1.267×10^{-8}
$\geq$1 mm	1120	2150	1.334×10^{-7}

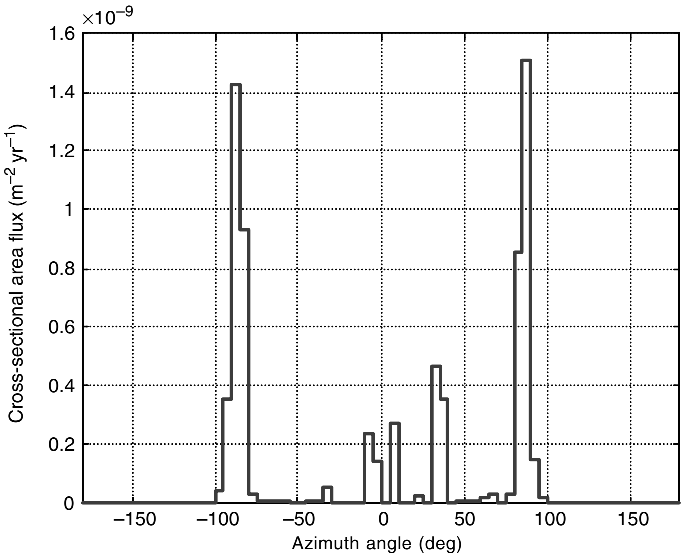

Figure 1. Background flux in GEO, as a function of azimuth, of debris $\geq$10 cm.

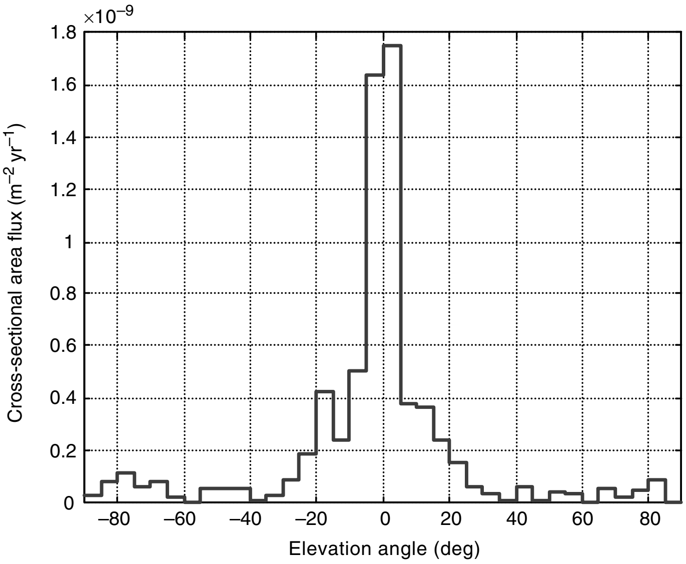

Figure 2. Background flux in GEO, as a function of elevation, of debris $\geq$10 cm.

The vector characteristics of the flux, highlighted in Figures 1–3, basically depend on four populations of objects:

1. Objects in near-synchronous orbit with inclinations $\leq 15^\circ$.
2. Objects in low inclination ($<30^\circ$) geostationary transfer orbits.
3. Objects in high inclination ($>40^\circ$) geostationary transfer orbits.
4. Objects in drifting (uncontrolled) Molniya orbits.

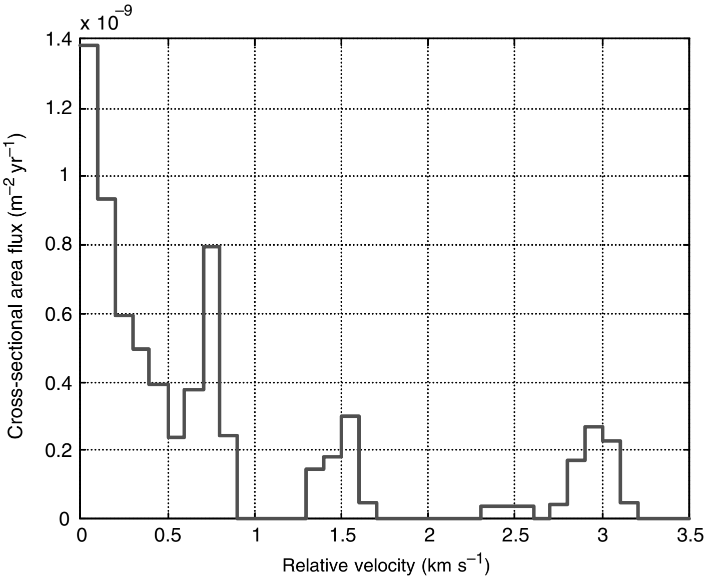

Figure 3. Background flux in GEO, as a function of relative velocity, of debris $\geq$10 cm.

These four groups of satellites can be easily identified in Figure 3, which presents the cross-sectional area flux in GEO as a function of the relative velocity. The objects in near-synchronous orbit are grouped below 900 m s^{-1}, those in low inclination geostationary transfer orbits are found at around 1.5 km s^{-1}, those in high inclinations geostationary transfer orbits, coming from Baikonur launches, are found at around 2.5 km s^{-1} and those in drifting Molniya orbits account for the peak around 3 km s^{-1}. A similar correspondence can be drawn from the peaks appearing in Figures 1 and 2, taking into due account the relative orbit geometry.

4. The Effect of a Satellite Explosion in Geostationary Orbit

The simulated low intensity explosion in GEO produced a sizable amount of fragments affecting the GEO ring. Immediately after the event, the average debris cross-sectional area flux on a geostationary spacecraft was 2.53×10^{-8}, 2.37×10^{-8} and 9.85×10^{-9} m^{-2} yr^{-1}, respectively, for particles larger than 1 mm, 1 and 10 cm. These values were approximately one-fifth of the debris background for particles greater than 1 mm, while the flux due to centimeter and decimeter sized fragments was higher, respectively, by 90% and 50% with respect to the background population.

Figures 4–6 show the cross-sectional area flux in GEO due to the fragments larger than 10 cm generated by the simulated explosion, as a function, respectively, of the azimuth, elevation and relative velocity. An average impact velocity smaller than 100 m s^{-1} was obtained. Moreover, it is worth noting the almost omnidirectional debris flux (Figures 4 and 5), due to the substantial isotropy of the simulated explosion, to the comparatively sizable velocity increment of the fragments with respect to the orbital velocity at geosynchronous altitude

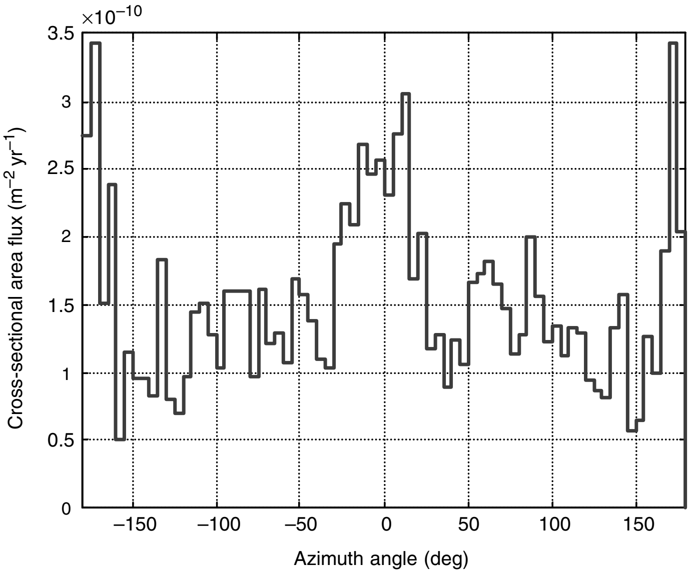

Figure 4. Flux of debris ≥10 cm in GEO, as a function of azimuth, due to an explosion in GEO (explosion elapsed time = 0 yrs).

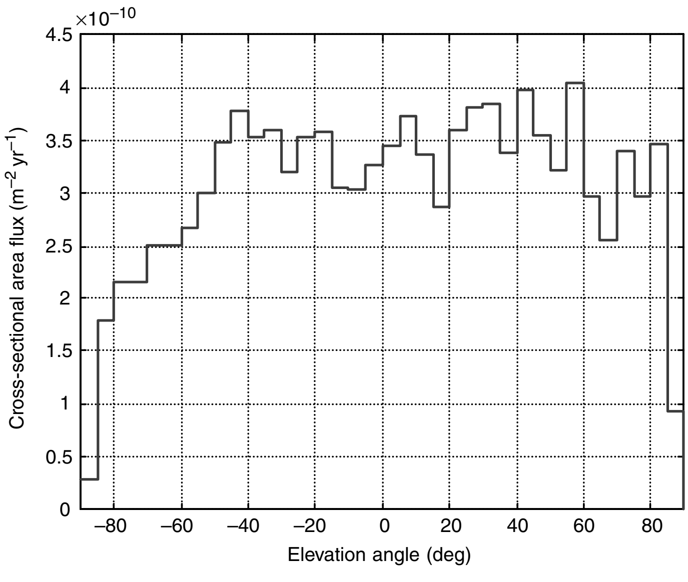

Figure 5. Flux of debris ≥10 cm in GEO, as a function of elevation, due to an explosion in GEO (explosion elapsed time = 0 yrs).

and to the resulting relative velocity vectors between the fragments and a generic target spacecraft in GEO.

In less than one year, the flux of fragments greater than 1 and 10 cm was also found to decrease below that of the background environment, due mainly to the luni-solar attraction.

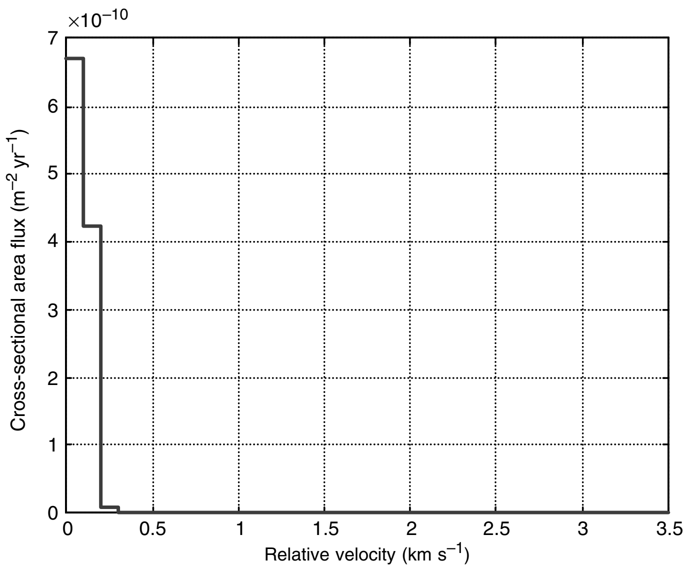

Figure 6. Flux of debris $\geq$10 cm in GEO, as a function of relative velocity, due to an explosion in GEO (explosion elapsed time = 0 yrs).

However, in the long term, it stabilized at around 1.7×10^{-9} m^{-2} yr^{-1}, for centimeter sized particles, and at around 10^{-9} m^{-2} yr^{-1}, for decimeter sized debris, with a residual modulation of 30–50% due to the orbital perturbations. These results mean that 6–7 additional low intensity explosions in GEO would be sufficient, in the long term, to double the current collision risk in the GEO ring with objects larger than 1 and 10 cm.

Even though the average flux was found to have almost stabilized 5 yrs after the simulated explosion, the effect (mainly) of the luni-solar perturbations led to dramatic changes in the debris cloud orbital geometry, modifying the 'quality' of its interaction with the GEO ring, as summarized, for the fragments larger than 10 cm, by Figures 7–9 (24 yrs after the explosion) and Figures 10–12 (54 yrs after the explosion).

5. Effects of Explosions above the Geostationary Ring

The time evolution of the average cross-sectional area flux on the GEO ring due to spacecraft explosions at and above the geostationary altitude is shown in Figures 13–15 for, respectively, debris larger than 1 mm, 1 and 10 cm. Figure 16 presents the time evolution of the average impact velocity only for the decimeter sized fragments, but the results obtained for smaller particles were very similar.

The variation of the debris density, relative velocity and average impact velocity (Figure 16), as well as that of the directional properties of the flux (see Figures 4–12 for the explosion in GEO), is a direct consequence of the debris orbital plane evolution, with a period T of about 54 yrs, due mainly to the luni-solar perturbations. Smaller debris density oscillations in GEO, with periods in between 27 yrs and one month, are the result of the luni-solar attraction and the low degree and order tesseral harmonics of the geopotential,

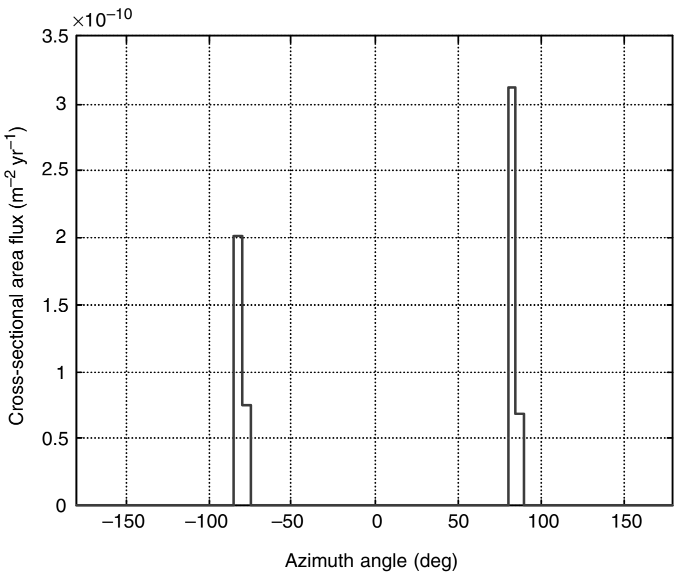

Figure 7. Flux of debris $\geq$10 cm in GEO, as a function of azimuth, due to an explosion in GEO (explosion elapsed time = 24 yrs).

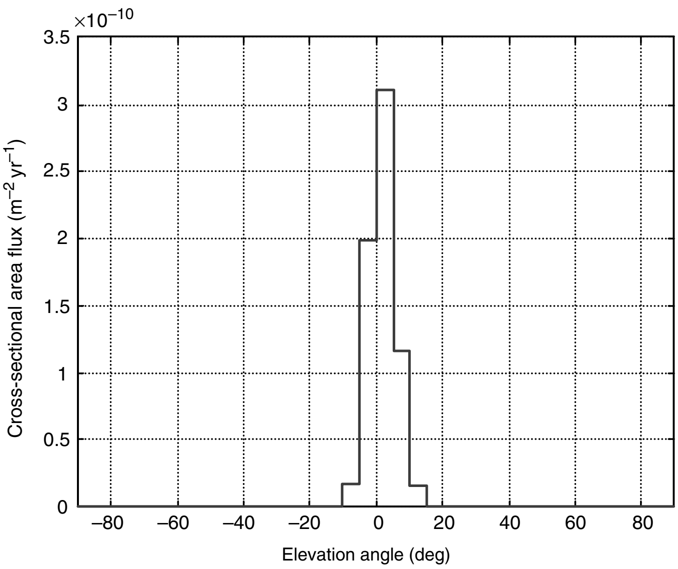

Figure 8. Flux of debris $\geq$10 cm in GEO, as a function of elevation, due to an explosion in GEO (explosion elapsed time = 24 yrs).

while the solar radiation pressure only plays a non-negligible role in the trajectory of the smaller particles.

However, the density and relative velocity changes are out of phase by π (i.e., 27 yrs). The overall resulting effect is the approximate long-term stabilization of the debris flux F

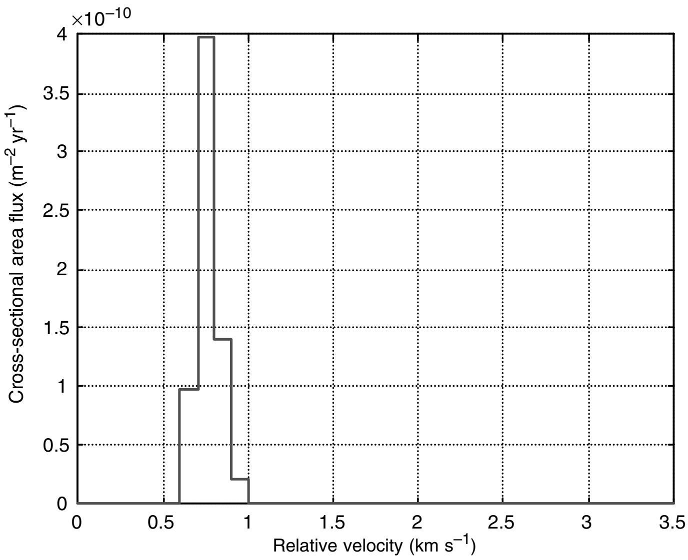

Figure 9. Flux of debris ≥ 10 cm in GEO, as a function of relative velocity, due to an explosion in GEO (explosion elapsed time = 24 yrs).

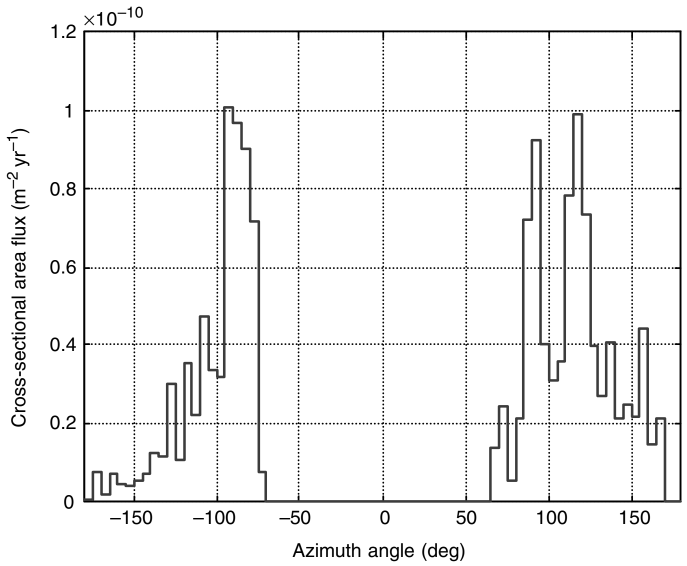

Figure 10. Flux of debris ≥ 10 cm in GEO, as a function of azimuth, due to an explosion in GEO (explosion elapsed time = 54 yrs).

in the GEO ring, occurring less than 6 yrs after the simulated fragmentation, irrespective of the explosion altitude, according to the relationship

$$F \approx K_0 + K_1 \cos\left(\frac{2\pi}{T}t\right) + K_2 \cos\left(\frac{4\pi}{T}t\right), \tag{2}$$

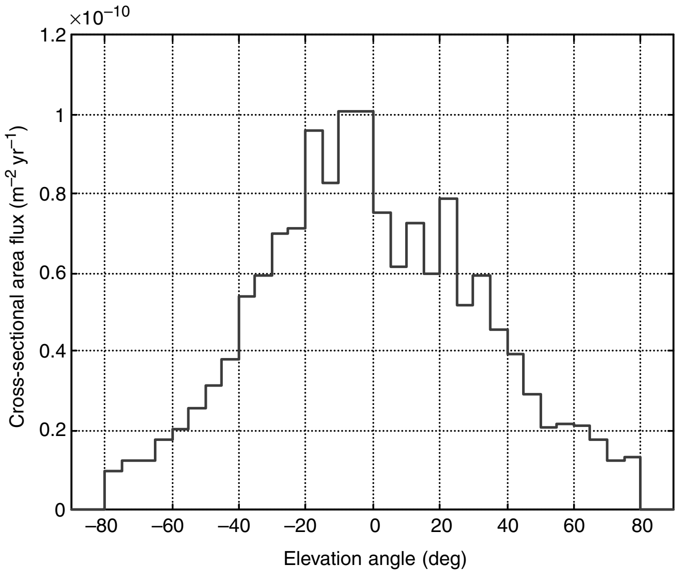

Figure 11. Flux of debris ≥10 cm in GEO, as a function of elevation, due to an explosion in GEO (explosion elapsed time = 54 yrs).

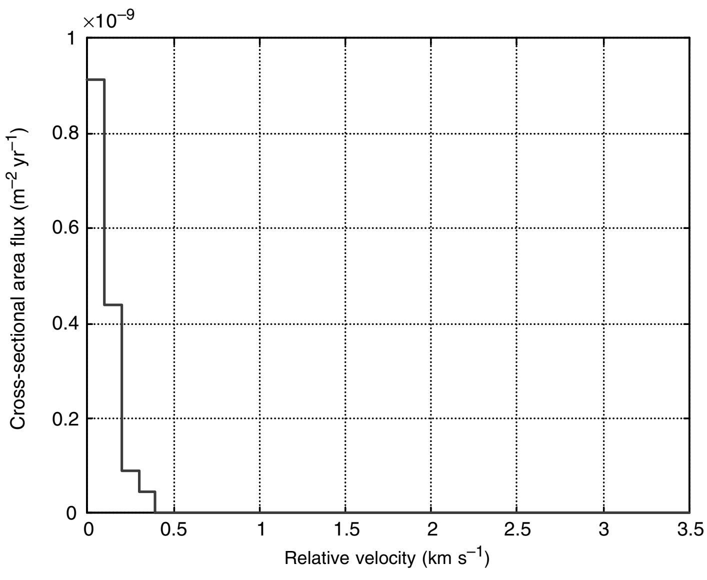

Figure 12. Flux of debris ≥10 cm in GEO, as a function of relative velocity, due to an explosion in GEO (explosion elapsed time = 54 yrs).

where t is the explosion elapsed time and K_0, K_1 and K_2 are three constants. They are functions of the breakup characteristics and altitude. Relatively small oscillations, due to the lunar nodal regression ($T \approx 18.6$ yrs), the advance of the lunar line of apsides ($T \approx 8.9$ yrs), the tesseral harmonics of the geopotential ($T \approx 3$ yrs) and so forth,

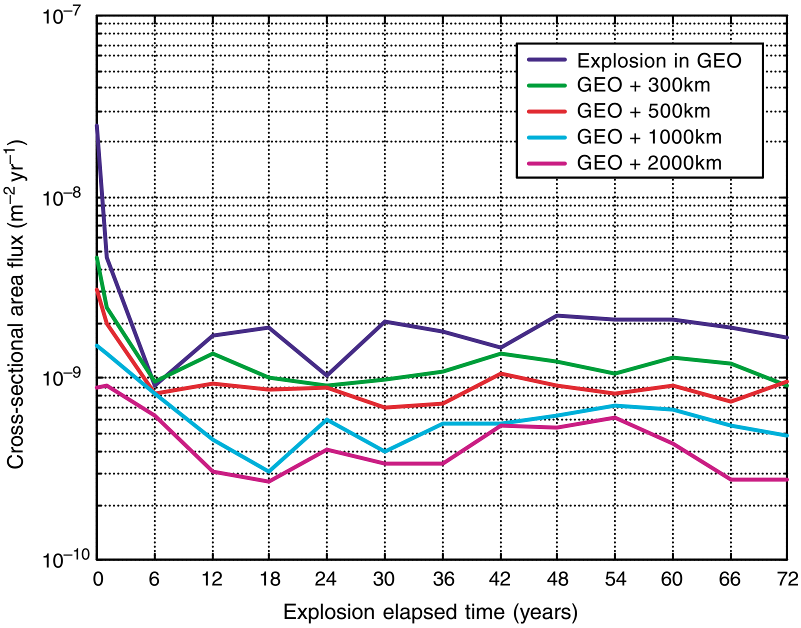

Figure 13. Flux of explosion fragments ≥ 1 mm in GEO, as a function of the breakup altitude and elapsed time.

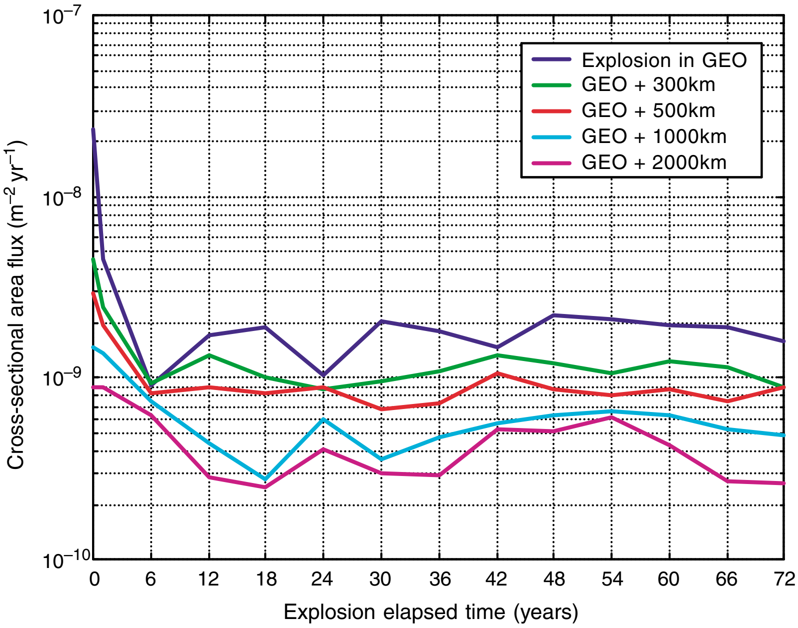

Figure 14. Flux of explosion fragments ≥ 1 cm in GEO, as a function of the breakup altitude and elapsed time.

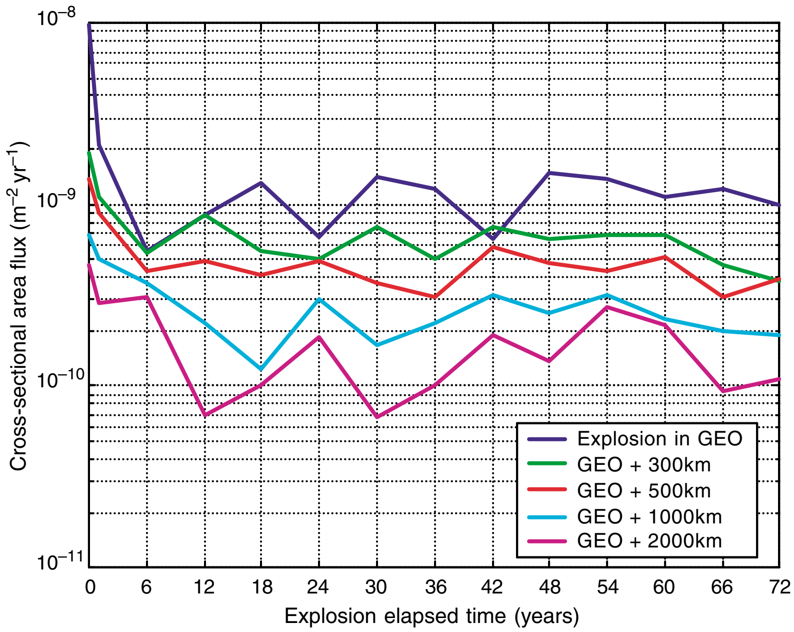

Figure 15. Flux of explosion fragments ≥10 cm in GEO, as a function of the breakup altitude and elapsed time.

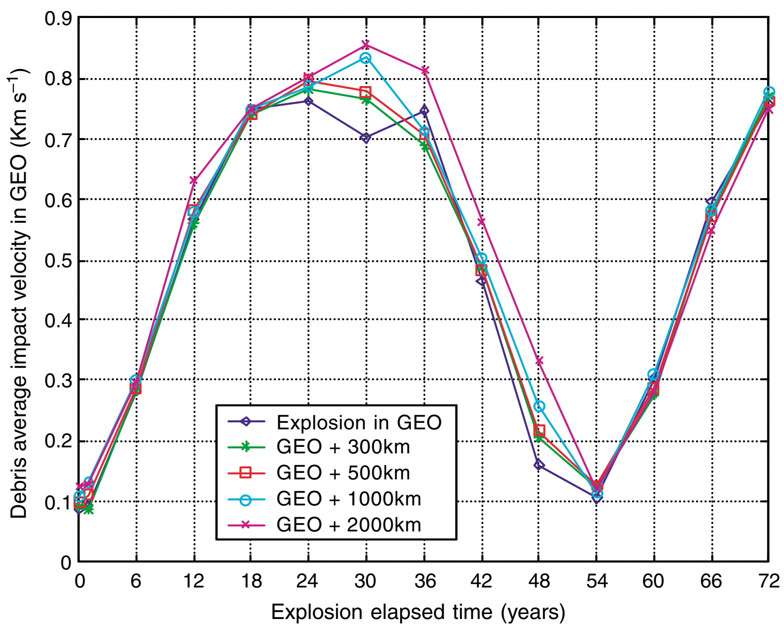

Figure 16. Time evolution of the debris average impact velocity in GEO as a function of the explosion altitude.

were superimposed on the general trend of the long-term debris flux approximated by Eq. (2).

Even for the explosions above the geostationary altitude, the same general patterns found for the fragmentation in GEO were observed (Figures 13–15), but with a reduction of the debris flux in the GEO ring due to increasing breakup altitudes. The explosion that was simulated 300 km above GEO (an altitude close to the one obtained by applying Eq. (1) to typical communication satellites), produced, immediately after the event, an average debris cross-sectional area flux on the GEO ring of 4.69×10^{-9}, 4.46×10^{-9} and 1.94×10^{-9} m^{-2} yr^{-1}, respectively, for particles larger than 1 mm, 1 and 10 cm. These values were approximately 1/30 of the debris background for particles greater than 1 mm and about 1/3 of the background for centimeter and decimeter sized fragments.

Within a few years, the flux dropped to a long-term equilibrium value close to 10^{-9} m^{-2} yr^{-1}, for particles larger than 1 cm, and to 6×10^{-10} m^2 yr^{-1}, for fragments greater than 10 cm, modulated by the above-mentioned oscillations, with a maximum total amplitude of 20–40%. These results demonstrate that about 10 explosions of typical spacecraft, at the end-of-life re-orbit altitude recommended by IADC, would be sufficient to double the average flux, in the GEO ring, of debris larger than 1 and 10 cm, thus matching the effect of the existing background, as represented by CODRM-99. An increase in the re-orbit altitude to 500 km would not significantly improve the situation (the long-term equilibrium flux obtained was smaller by just 20–30%), as shown in Figures 13–15.

To reduce by one order of magnitude the long-term average flux of explosion fragments larger than 10 cm with respect to the breakup in the GEO, a re-orbiting altitude at least 2000 km above GEO should be used. In that case, about 100 spacecraft catastrophic explosions would be needed to produce an additional debris flux on the GEO ring comparable to the existing background, as modeled by CODRM-99. However, for centimeter sized particles, the same threshold would be reached with approximately one-third of the breakups.

6. Conclusions

The short- and long-term effects of spacecraft explosions, as a function of the end-of-life re-orbiting altitude (0–2000 km) above the GEO, were analyzed in terms of the additional contribution to the debris flux in the GEO ring. The simulated clouds of fragments were propagated with a high precision trajectory integration code, taking into account all the relevant orbital perturbations.

In the altitude range considered, the fragments produced by the different explosions show a similar evolution of the average relative and impact velocity (Figure 16) with respect to a satellite in GEO. Their relative contribution to the collision risk in the GEO ring is, therefore, mainly a function of the average fragment density there and, as expected, the explosion in GEO turned out to be the most detrimental for the GEO environment (Pardini and Anselmo, 2001).

The results obtained show that 6–7 additional low intensity explosions in GEO would be sufficient, in the long term, to double the current collision risk in the GEO ring with objects larger than 1 and 10 cm. Unfortunately, even the adoption of the end-of-life re-orbiting recommended by IADC, resulting, for typical satellites, in an altitude increase in between 300 and 500 km, would not improve the situation much, because even just a dozen explosions would be sufficient to double the average flux of debris larger than 1 and 10 cm, thus matching the effect of the existing background, as modeled by CODRM-99. To significantly reduce the long-term average flux of explosion fragments larger than 10 cm, a re-orbiting altitude at least 2000 km above GEO should be used. In that case, about 100 breakups would be necessary in order to produce an additional debris flux on the GEO ring comparable to the existing modeled background.

In conclusion, the optimal debris mitigation strategy in GEO should be a compromise between spacecraft end-of-life passivation effectiveness, spacecraft end-of-life re-orbiting altitude, and the acceptable debris background in the GEO ring. If the goal of the international community of space agencies and operators is to preserve the existing background, the recommended end-of-life re-orbiting altitude would depend critically on the level of application, reliability and effectiveness of satellite passivation and long-term explosion avoidance. Therefore, the re-orbiting altitude endorsed by IADC would only be adequate if satellite passivation was extensively and successfully carried out, as recommended by IADC as well. However, if this were not the case, higher re-orbiting altitudes would have to be considered.

Acknowledgements

The authors contributed to this paper in the framework of the Cooperation Agreement (1997–2001) between the CNUCE Institute of the National Research Council (CNR) and the Italian Space Agency (ASI).

References

J.L. Africano and T. Schildknecht. *International Geostationary Observation Campaign*. Report for AI-12.1, IADC-00-04, Inter-Agency Space Debris Coordination Committee (IADC), 2000.

L. Anselmo and C. Pardini. The Effects of Spacecraft and Upper Stage Breakups on the Geostationary Ring. *The Journal of the Astronautical Sciences*, 48: 1–23, 2000.

V.A. Chobotov. Disposal of Spacecraft at End-of-Life. In *Geosynchronous Orbit, in Astrodynamics 1989, AAS Advances in the Astronautical Sciences*, Vol. 71, Univelt Inc., San Diego, California, pages 377–391, 1990.

W. Flury et al. Searching for Small Debris in Geostationary Ring – Discoveries with the Zeiss 1-metre Telescope. *ESA Bulletin*, 104: 92–100, 2000.

G. Fusco and A. Buratti. *Crowding of the Geostationary Orbit*. Final Report, ESA Contract No. 5705/83/NL/PP (SC), RIPTO, Turin, Italy, 1984.

M. Hechler and J.C. Van der Ha. Probability of Collisions in the Geostationary Ring. *Journal of Spacecraft and Rockets*, 18: 361–366, 1981.

Inter-Agency Space Debris Coordination Committee (IADC). *Space Debris Issues in the Geostationary Orbit and the Geostationary Transfer Orbits*. Presented to the 37th Session of the Scientific and Technical Subcommittee, Committee on the Peaceful Uses of Outer Space, United Nations, Vienna, Austria, 2000.

K. Jorgensen et al. Optical Observations of Geosynchronous Debris. In *52nd International Astronautical Congress*, 1–5 October, Toulouse, France, Paper IAA-01-IAA.6.4.03, 2001.

J.H. Kwok. *The Artificial Satellite Analysis Program (ASAP)*. Version 2.0, JPL NPO-17522, Pasadena, California, USA, 1987.

C. Pardini. *Development of a Single Fragmentation Event Simulator (CLDSIM)*. Study Note of Work Package 3600, Study on Long Term Evolution of Earth Orbiting Debris, ESA/ESOC Contract No. 10034/92/D/IM(SC), Consorzio Pisa Ricerche, Pisa, Italy, 1995.

C. Pardini. *Model for the Initial Population*. Study Note of Work Package 1, Space Debris Mitigation: Extension of the SDM Tool, ESA/ESOC Contract No. 13037/98/D/IM, Consorzio Pisa Ricerche, Pisa, Italy, 2000.

C. Pardini and L. Anselmo. Assessing the Risk of Orbital Debris Impact. *Space Debris*, 1: 59–80, 1999.

C. Pardini and L. Anselmo. SDIRAT: Introducing a New Method for Orbital Debris Collision Risk Assessment. In *Proceedings of the International Symposium on Space Dynamics*, June 26–30, 2000, Biarritz, France, Paper MS00/23, pages 1–9, 2000.

C. Pardini and L. Anselmo. On the Effectiveness of End-of-Life Re-Orbiting for Debris Mitigation in Geostationary Orbit. *Space Debris*, 1: 173–193, 2001.

C. Pardini, L. Anselmo, A. Rossi, A. Cordelli and P. Farinella. A New Orbital Debris Reference Model. *The Journal of the Astronautical Sciences*, 46: 249–265, 1998.

R.C. Reynolds. Review of Current Activities to Model and Measure the Orbital Debris Environment in Low-Earth-Orbit. *Advances in Space Research*, 10: 359–372, 1990.

T. Schildknecht et al. Optical Survey for Space Debris in GEO. In *52nd International Astronautical Congress*, 1–5 October, Toulouse, France, Paper IAA-01-IAA.6.4.02, 2001.

S.Y. Su and D.J. Kessler. Contribution of Explosion and Future Collision Fragments to the Orbital Debris Environment. *Advances in Space Research*, 5: 25–34, 1985.